A First Order Model Based Control of a Hydraulic Seismic Isolator Test Rig

S. Strano and M. Terzo

Abstract— **This paper presents the design of an adaptive control of a hydraulic seismic isolator testing machine. The system exhibits dead zone, frictions and parametric uncertainty due to both the operating conditions and the unknown features of the device to be tested. A system structure identification is described and a first order non-linear model is obtained. Adopting the first order system as nominal one, the synthesis of a model reference adaptive control is carried out. The illustrated simulation results show the effectiveness of the proposed approach.**

Index Terms— **control, hydraulic actuator, parametric uncertainty, seismic isolator, shaking table, system structure identification**

I. Introduction

The paper describes an experimental/theoretical activity carried out on a hydraulically actuated shaking table employed as seismic isolator test rig. The isolators to be tested are adopted in the base isolation strategies which are functional to mitigate structural responses under strong external excitations, such as earthquakes and wind storms. Passive and semi-active isolators have to be opportunely tested in order to evaluate their characteristics in terms of restoring force and energy loss. To this end, these devices are tested in order to obtain the force-displacement cycle that allows an analytical description of their dynamic characteristics to be deduced [1]. Hydraulic actuators are typically characterized by parametric uncertainty due to the influence of the operating conditions on the parameter values. Consequently, traditional shaking-table testing has been limited by the effectiveness of conventional fixed-gain algorithms used in their control. Furthermore, in addition to the described features, the employment of a hydraulically actuated shaking table as isolator test rig involves an additional and more incisive source of parametric uncertainty caused by the presence of the isolator under test (IUT) which characteristics are fully unknown. Such a devices are characterized by features that can be very different for each pattern and depending, principally, on the structure that has to be isolated. So, the change of the IUT implies a modification in the system to be controlled and this has to be considered in the controller synthesis.

In the following, a theoretical-experimental activity, carried out on a seismic isolator test rig, is described. The test rig mainly consists of a sliding table, driven by a hydraulic cylinder, on which the IUT is connected; the other end of the isolator is connected to a reaction structure. In this paper, a model reference adaptive control is designed. By means of system structure identification technique, a simplified model, functional for controller synthesis, is derived. Starting from experimental data, the structure of a first order non-linear system [2 - 5], with parameters depending on both the operating conditions and the IUT, is identified. The theoretical-experimental comparisons confirm the soundness of the proposed first order non-linear model (1^{st}OM) which can be assumed for the controller design. The parametric uncertainty suggests the employment of an adaptive control which typically improves its performance as adaptation goes on and needs for each test no parameter identification nor tuning procedure that are limited in scope by the expertise of the operator. Starting from the 1^{st}OM, a model reference adaptive control is synthesized. The designed adaptive non-linear control has been tested by means of numerical simulations carried out on the validated fifth order non-linear model (5^{th}OM) of the test rig and in presence of different IUT. The numerical results confirm the effectiveness of the proposed algorithm.

II. Test Rig Description and Modelling

The test rig (Fig. 1, 2) consists of a fixed base, a hydraulic actuator and a sliding table [6 - 9]. The table motion is constrained to a single horizontal axis by means of linear guides. The isolator under test is placed between the sliding table (A) and the vertical slide (B) (Fig. 1).

The hydraulic jack (C) allows the isolator under test (Fig. 2) to be vertically loaded (max 850 kN). The jack load and the force acting on the table are balanced by the vertical (D) and horizontal (E) reaction structures respectively.

The hydraulic power unit consists of an axial piston pump powered by a 75 kW AC electric motor. The pump is characterized by a variable displacement in the range 70-140 cm3 and it is able to generate a maximum pressure of 210 bar and a maximum flow rate equal to 313 l/min. A pressure relief valve is located downstream of the pump.

Eq. (1) consists into the test rig mathematical model in which no isolator is installed: the hydraulic cylinder has to move the sliding table only.

S. Strano is with the *Dipartimento di Ingegneria Industriale*, *Università degli Studi di Napoli Federico II*, Napoli, 80125 ITALY (e-mail: salvatore.strano@unina.it).

M. Terzo is with the *Dipartimento di Ingegneria Industriale, Università degli Studi di Napoli Federico II*, Napoli, 80125 ITALY, (corresponding author, phone: +390817683285; fax: +390812394165; e-mail: m.terzo@unina.it).

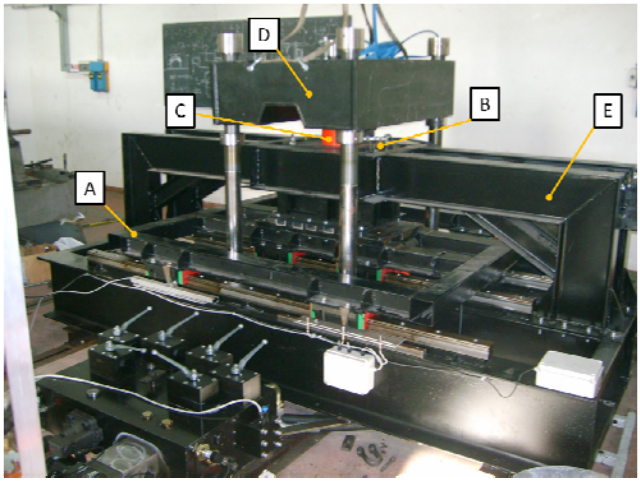

Fig. 1. Test rig

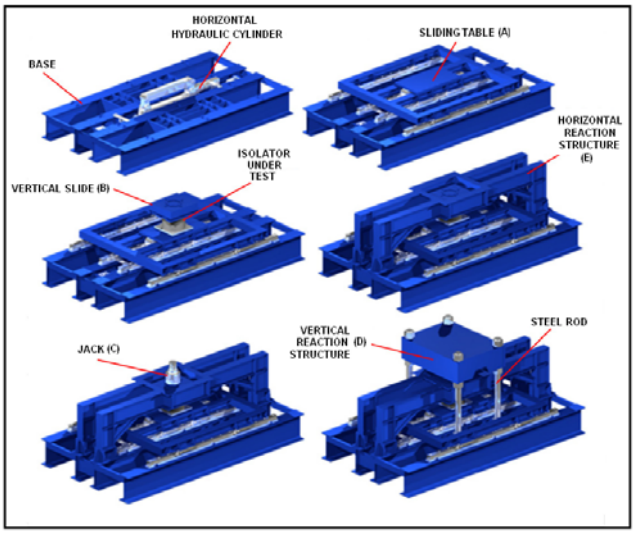

Fig. 2. Test rig components

$$\begin{cases} m\ddot{y} + (\mu N + F_c)\,\mathrm{sgn}(\dot{y}) + \sigma\dot{y} = A_p P_L \\ \dfrac{V_0}{2\beta}\dot{P}_L = -A_p\dot{y} + Q_L \\ Q_L = DZ(v_e)\sqrt{P_s - \mathrm{sgn}(v_e)P_L} \\ \ddot{v}_e = -\omega_{nv}^2 v_e - 2\xi_v\omega_{nv}\dot{v}_e + \omega_{nv}^2 v_c \end{cases} \quad (1)$$

where:
y=table displacement;
m=movable mass;
N=vertical load on the linear guides;
μ=Coulombian friction coefficient;
σ=viscous friction coefficient;
F_c=Coulomb friction force;
A_p=piston area;
P_L =load pressure;
Q_L=load flow;
V_0=oil volume between the piston and the valve in each side for the centered barrel position;
β=effective Bulk modulus;
v_e=voltage signal proportional to the valve spool position x_v;
$DZ(v_e)$=dead zone function;
P_S=supply pressure;
v_c =valve command voltage due to its electronic driver;
ω_{nv}=natural frequency of the valve;
ξ_v= damping ratio of the valve;

The relationship between v_c and the control action u is:

$$v_c = \begin{cases} k_{ep}u + v_{e0} & if \quad u > 0 \\ v_{e0} & if \quad u = 0 \\ k_{en}u + v_{e0} & if \quad u < 0 \end{cases} \quad (2)$$

In order to take the IUT into account in the mathematical model, the restoring force has to be considered in the first equation of (1).

So, the isolator test rig can be completely modelled by the following Eq. (3) (5thOM):

$$\begin{cases} m\ddot{y} + (\mu N + F_c)\,\mathrm{sgn}(\dot{y}) + \sigma\dot{y} + F_{BW} = A_p P_L \\ \dfrac{V_0}{2\beta}\dot{P}_L = -A_p\dot{y} + DZ(v_e)\sqrt{P_s - \mathrm{sgn}(v_e)P_L} \\ \ddot{v}_e = -\omega_{nv}^2 v_e - 2\xi_v\omega_{nv}\dot{v}_e + \omega_{nv}^2 v_c \end{cases} \quad (3)$$

in which F_{BW} is the isolator restoring force.

A. *Seismic isolator modelling*

The isolator restoring force (F_{BW}) has been modelled by the Bouc-Wen law. The model consists of Eq. (4).

$$F_{BW}(t) = k_d d(t) + k_w w(t)$$
$$\dot{w}(t) = \rho_{BW}\dot{d}(t)\left\{1 + |w(t)|^n \sigma_{BW}\left[1 - \mathrm{sgn}(\dot{d}(t)w(t)) - \frac{1}{\sigma_{BW}}\right]\right\} \quad (4)$$

where $d(t)$ is the time history of the isolator deformation (assumed equal to the table displacement); k_d, k_w, σ_{BW}, ρ_{BW} and n are the Bouc-Wen model parameters that determine the shape of the hysteretic cycle.

Two different seismic isolators (in the following indicated with "IUT_a" and "IUT_b" respectively) have been considered in the described activity. They are commonly employed in seismic isolation and are characterized by different characteristics because of elastomeric layers and reinforcements. The Bouc-Wen model parameters have been identified starting from experimental data. Fig. 3 and 4 show the comparison between an experimental hysteretic cycle and the simulated one for the IUT_a and IUT_b respectively.

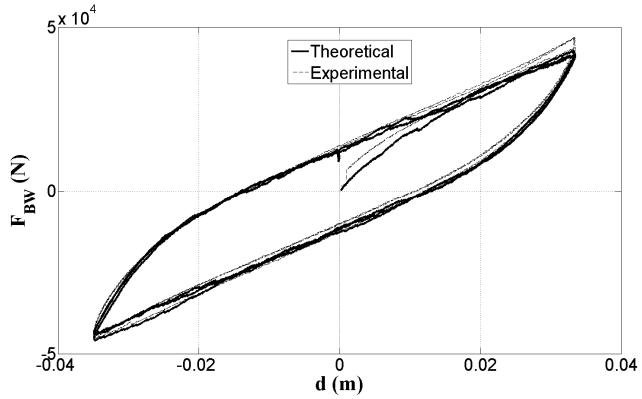

Fig. 3 . Experimental and simulated hysteretic cycles for IUT_a

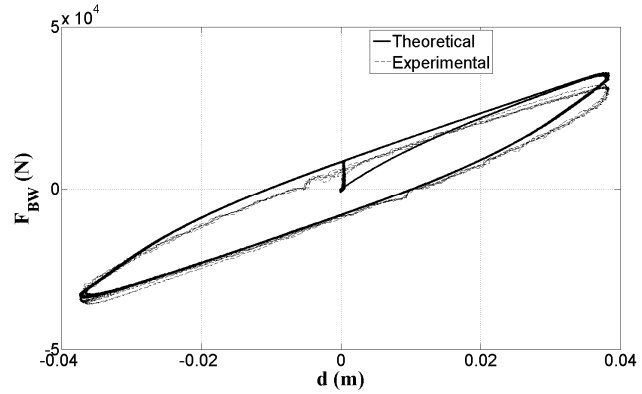

Fig. 4. Experimental and simulated hysteretic cycles for IUT_b

The identified parameters of the IUT_a and IUT_b are illustrated in Table I and II respectively.

TABLE I
BOUC-WEN MODEL PARAMETERS OF THE IUT_a

Bouc-Wen model parameter	ρ_{BW}	σ_{BW}	n	k_d	k_w
Value	141	0.5	1	1.25e6	1.7e4
Unit	1/m	-	-	N/m	N

TABLE II
BOUC-WEN MODEL PARAMETERS OF THE IUT_B

Bouc-Wen model parameter	ρ_{BW}	σ_{BW}	n	k_d	k_w
Value	90	0.5	1	6.8e5	6.2e3
Unit	1/m	-	-	N/m	N

The shape of the hysteretic cycles and the identified parameters confirm the differences, in terms of their characteristics, between the two isolators.

III. SIMPLIFIED MODEL DERIVATION FOR CONTROLLER SYNTHESIS

Large figures and tables may span both columns. Place In the present section, a system simplified model (1stOM) is derived by means of identification technique starting from experimental data observation. The basic idea consists in the possibility of modelling the isolator test rig as a first order model and then employ it in an adaptive control design which can be able to enhance the control performances in different operative conditions and in presence of isolators with different characteristics. Some considerations can be made to physically justify the possibility of modelling the isolator test rig as a first order model. With the assumption of neglecting the dynamics of both the load pressure and the valve spool respect to the table one, the system (3) reduces in a second order differential equation. Beside, taking into account the typical frequencies employed in the isolator testing [10], inertial forces can be neglected in the first equation of the system (3). As a consequence, a single first order differential equation in the variable y can be adopted as a simplification of the system (3). Experimental evidence allows to verify the cited hypothesis.

The Fig. 5 and 6 illustrate the test rig displacement obtained in presence of the step signal as input and a supply pressure of 40 bar for the two different isolators introduced above.

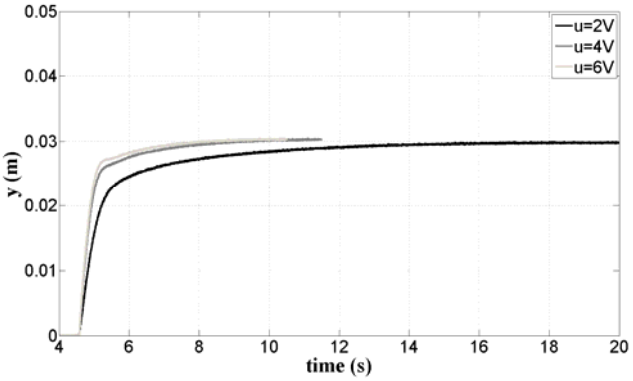

Fig. 5. Experimental step response of the isolator test rig in presence of the IUT_a

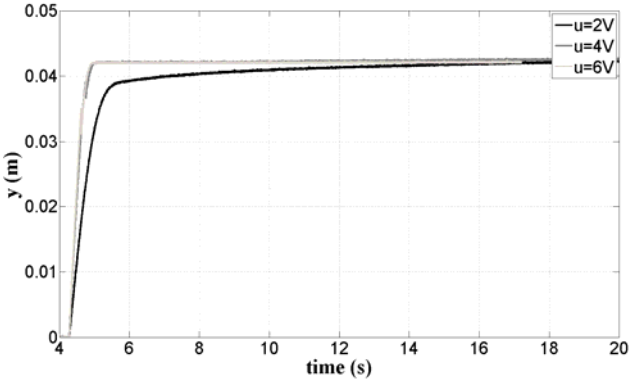

Fig. 6. Experimental step response of the isolator test rig in presence of the IUT_b

The possibility of the employment of a reduced order system for the modelling of the isolator test rig is confirmed by the experimental step response. Indeed, the observation of the plant dynamic behaviour clearly exhibits the property of being well approximated by a first order system [11]. By means of an identification technique, a state space system structure can be derived and then employed for an adaptive control synthesis.

The illustrated experimental evidence shows the transient and the steady state system properties. As regards the transient behaviour, a slight difference can be appreciated for the step input characterized by an amplitude of 2 V.

The steady state test rig response has to be analyzed in

order to execute the system structure identification. The steady state value of the test rig displacement (Fig. 5 and 6) is not influenced by the input amplitude and this highlights a highly non-linear behaviour. Taking the test rig step response into account, the amplitude of the input voltage in correspondence of three values of the settling displacement can be represented for both the IUT (Fig. 7 and 8). In order to execute the system structure identification, a fit (5) that well approximates the steady state response is showed.

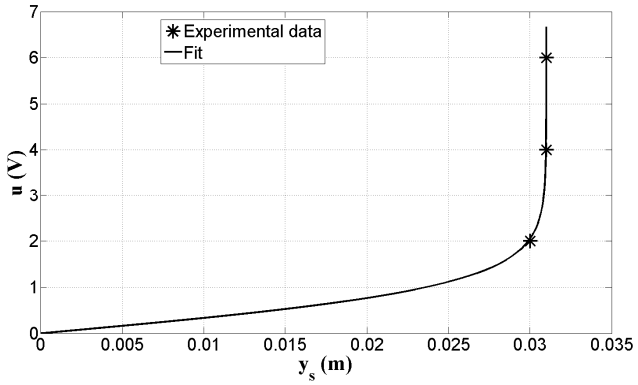

Fig. 7. Steady state response and proposed fit in presence of the IUT_a

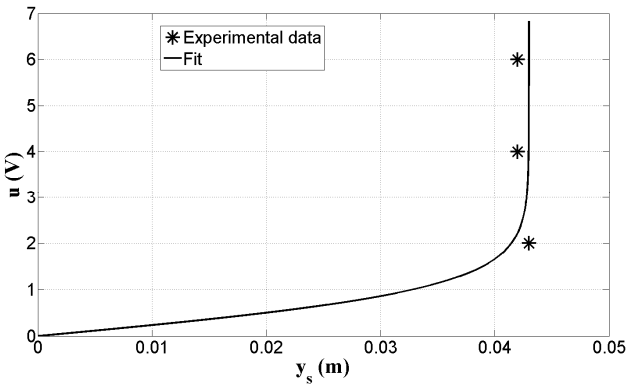

Fig. 8. Steady state response and proposed fit in presence of the IUT_b

$$u = k\ tanh^{-1}(\frac{y_s}{a_s}) \tag{5}$$

The proposed fit (5) is functional to reproduce the steady state non-linear behaviour of the system consisting in an insensitiveness of the settling displacement respect to the input voltage. The parameter k is characterized by voltage dimension and unitary value, while the parameter a_s consists, in practice, in the steady state displacement value. As it will be seen after, the parameter a_s is clearly influenced by the supply pressure P_s and the IUT.

The introduced fit allows the following steady state system structure (6), in the state-space form, to be proposed:

$$y_s = \frac{y_s}{k\ tanh^{-1}(\frac{y_s}{a_s})}u \tag{6}$$

Taking the first order dynamics into account, the identified system structure for the 1[st]OM is:

$$\dot{y} = -a_p y + \frac{a_p y}{k\ tanh^{-1}(\frac{y}{a_s})}u \tag{7}$$

The 1[st]OM response is compared (Fig. 9 and 10) with the experimental ones for both the IUT. A P_s of 40 bar and a step input voltage of 2V have been adopted.

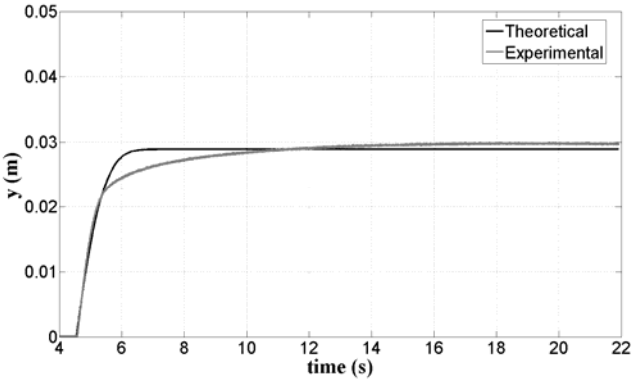

Fig. 9. Theoretical-experimental comparison in presence of the IUT_a

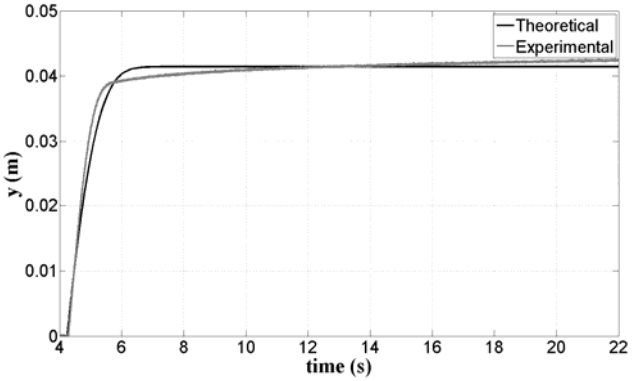

Fig. 10. Theoretical-experimental comparison in presence of the IUT_b

The result illustrated in Fig. 9 refers to a_p=0.51 s^{-1} and a_s=0.03 m while that showed in Fig. 10 to a_p=0.58 s^{-1} and a_s=0.043 m.

The proposed 1[st]OM (7) reproduces, with an acceptable approximation, the isolator test rig behaviour. Furthermore, the IUT typology doesn't affect the goodness of the identified system structure. The influence of both the supply pressure P_s and the isolator characteristics on model parameters will be evaluated in the following section.

A. Parameter sensitivity analysis

Experimental tests have been carried out in order to evaluate the influence of both supply pressure and isolator on model (7) parameters. The employed input voltage consists in step signal of amplitude 2, 4 and 6 V; three different values in terms of supply pressure P_s (20, 30 and 40 bar) and the two described isolators have been adopted.

The measured quantities have been sampled at 500 Hz and a parameter identification procedure has been realized by a non-linear least square algorithm applied to the input and output. The following tables show the identified parameters for each test. Table III and IV refer to IUT_a and IUT_b respectively.

The tests are named with respect to the following denotation:

$$P_s\mathrm{S}u\mathrm{T}$$

where S represents the supply pressure (bar) and T the amplitude (V) of the step signal adopted for the input voltage.

TABLE III
IDENTIFIED VALUES IN PRESENCE OF THE IUT_a

Test	a_p (s^{-1})	a_s (m)
P_s20u2	0.49	0.01
P_s20u4	0.55	0.011
P_s20u6	0.57	0.011
P_s30u2	0.49	0.021
P_s30u4	0.54	0.022
P_s30u6	0.56	0.022
P_s40u2	0.51	0.03
P_s40u4	0.56	0.031
P_s40u6	0.58	0.031

TABLE IV
IDENTIFIED VALUES IN PRESENCE OF THE IUT_b

Test	a_p (s^{-1})	a_s (m)
P_s20u2	0.6	0.016
P_s20u4	0.71	0.014
P_s20u6	0.72	0.015
P_s30u2	0.61	0.028
P_s30u4	0.72	0.027
P_s30u6	0.71	0.028
P_s40u2	0.58	0.043
P_s40u4	0.69	0.042
P_s40u6	0.7	0.042

With reference to the tests characterized by the same supply pressure and different input voltage, the parameter a_p appears varying very slowly while the parameter a_s is substantially constant. This result confirms the goodness of the identified non-linear structure that can be considered functional to well approximate the system behaviour. As regards the influence of the supply pressure, it is manifest on the parameter a_s, i.e. on the steady state value of the system output. The increasing of the supply pressure determines an increasing of the parameter a_s: this can be physically justified taking into account, for example, the experimental step response obtained for a step input of 2 V and three different supply pressure for both isolators (Fig. 11 and 12). For each IUT, the settling displacement of the test rig is clearly influenced by the supply pressure.

Both model parameters are influenced by the employed isolator as can be observed comparing Table III and IV. This is obviously caused by the different IUT characteristics which determine the parametric uncertainty.

The developed considerations allow to consider the following logical scheme for the simplified system model (1^{st}OM). It consists of a single input-single output non-linear system with supply pressure P_s and the IUT acting as modifying input (Fig. 13).

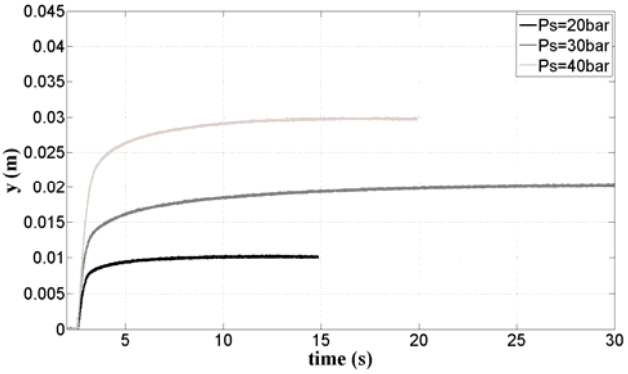

Fig. 11. Experimental step response in presence of the IUT_a

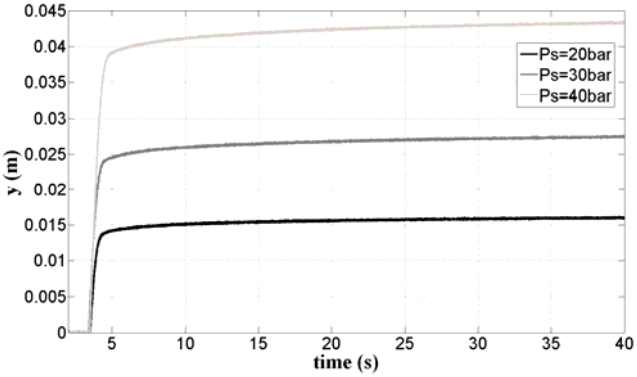

Fig. 12. Experimental step response in presence of the IUT_b

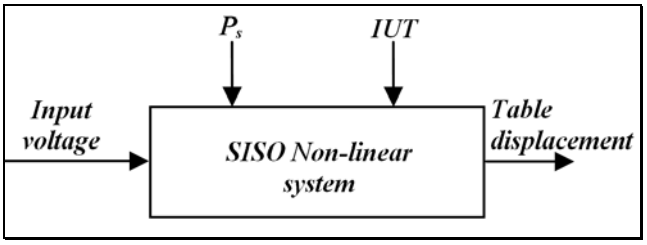

Fig. 13. Logical scheme of the test rig simplified model

The operative conditions and the typology of the IUT can significantly affect the model parameters. It follows a parameter uncertainty that suggests an adaptive approach for the control synthesis.

IV. Controller Design

The adaptive control is a feedback control method able to make the tracking error converge to zero in presence of a plant characterised by known structure and uncertain parameters. According to this approach, the table position measurement only is necessary for feedback control design [12].

With reference to the model reference adaptive control technique, the control scheme is illustrated below (Fig. 14).

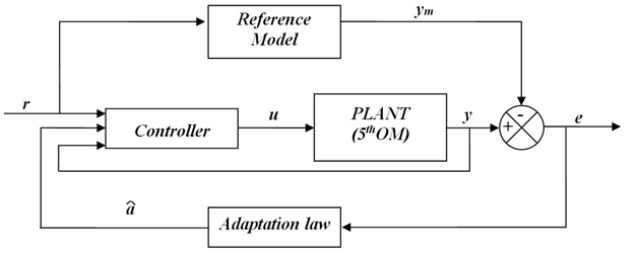

Fig. 14. Scheme of the model reference adaptive control

Where:
r = reference (target displacement)
y_m = reference model output
y = isolator test rig displacement
u= input voltage
e= y-y_m (tracking error)
$\hat{a}$ = adjustable controller parameters.

The control aims, by means of controller parameter adaptation, to make zero the error between the controlled system output (y) and the reference model output (y_m).

The 1stOM (7) of the plant has been considered for the adaptive control design. The model (7) is characterized by a known structure and parameters that are unknown for the control. The identified 1stOM allows the following reference model (14) to be considered:

$$\dot{y}_m = -a_m y_m + b_m r \tag{8}$$

The reference model is constituted by a linear first order SISO system characterised by the reference r as input, y_m as output, a_m and b_m fixed parameters. The following control action is proposed:

$$u = (\hat{a}_r r + \hat{a}_y y)\frac{k\ tanh^{-1}(y/\hat{a}_s)}{y} \tag{9}$$

with $\hat{a}_r$, $\hat{a}_y$ and $\hat{a}_s$ as adjustable controller parameters. The quantity $tanh^{-1}(y/\hat{a}_s)$ has been introduced with the intention of adaptively cancelling the system non-linear behaviour. Moreover, as the position y goes to zero, the feedback is numerically forced to an infinitesimal.

Substituting (9) in (7), the closed loop system equation is derived:

$$\dot{y} = -a_p y + \frac{a_p y}{tanh^{-1}(\frac{y}{a_s})}(\hat{a}_r r + \hat{a}_y y)\frac{tanh^{-1}(y/\hat{a}_s)}{y} \tag{10}$$

that can be written:

$$\dot{y} = -(a_p - a_p\hat{a}_y\chi)y + a_p\hat{a}_r\chi r \tag{11}$$

where $\chi = \dfrac{tanh^{-1}(y/\hat{a}_s)}{tanh^{-1}(y/a_s)}$

The tracking error dynamics can be defined by taking (8) and (11) into account:

$$\begin{aligned}\dot{e} = \dot{y} - \dot{y}_m &= -(a_p - a_p\hat{a}_y\chi)y + a_p\hat{a}_r\chi r + a_m y - a_m y + a_m y_m - b_m r = \\ &= -a_m(y - y_m) + (a_m - a_p + a_p\hat{a}_y\chi)y + (a_p\hat{a}_r\chi - b_m)r = \\ &= -a_m e + a_p\chi(\hat{a}_y + \frac{a_m - a_p}{a_p\chi})y + a_p\chi(\hat{a}_r - \frac{b_m}{a_p\chi})r\end{aligned} \tag{12}$$

It can be written:

$$\dot{e} = -a_m e + a_p\chi(\tilde{a}_y y + \tilde{a}_r r) \tag{13}$$

in which

$$\tilde{a}_y = \hat{a}_y + \frac{a_m - a_p}{a_p\chi} \tag{14}$$

$$\tilde{a}_r = \hat{a}_r - \frac{b_m}{a_p\chi} \tag{15}$$

The error dynamics can be conveniently expressed as:

$$e = \frac{a_p}{s + a_m}\chi(\tilde{a}_y y + \tilde{a}_r r) \tag{16}$$

in which s is the Laplace variable.

The tracking error consists into the response of a first order stable system ($a_m > 0$) subjected to the input:

$$\chi(\tilde{a}_y y + \tilde{a}_r r) \tag{17}$$

The identified system structure (7), together with the reference model (8) and the control action (9), give the tracking error dynamics (16) which allows the following adaptation laws to be used for controller parameters [13]:

$$\dot{\hat{a}}_s = -\gamma_{as} e\ tanh^{-1}(y) \tag{18}$$

$$\dot{\hat{a}}_y = -\gamma e y \tag{19}$$

$$\dot{\hat{a}}_r = -\gamma e r \tag{20}$$

with γ_{as} and γ being positive constant representing the adaptation gains.

The above adaptation laws allow the tracking error to converge to zero as the time t→∞.

V. Simulation results

Submission of a manuscript is not required for The adaptive controller, developed starting from the reduced order system (1stOM), has been tested on the 5thOM (3) which parameters, identified starting from experimental data, are unknown to the adaptive controller (Fig. 14). Parameters showed in Table I and II have been employed for IUT_a and IUT_b respectively. The model reference parameters are chosen to be:

a_m =50 s^{-1}; b_m =50 s^{-1}.

The adaptation gains γ_{as} and γ are chosen to be 2 and 1e5 respectively.

Taking the amplitude of the target displacement that will be assigned into account, the initial value of $\hat{a}_s$ has been fixed to 0.04. Initial values of $\hat{a}_y$ and $\hat{a}_r$ have been fixed

both to zero, indicating no *a priori* knowledge. The adaptation mechanism ensures that the controller minimizes the tracking error by means of the controller parameters adaptation. The initial conditions of the plant and reference model are both zero.

In the executed simulations, the vertical load on the specimen of 1.25×10^5 N has been imposed. A supply pressure P_s of 100 and 70 bar have been adopted for the test of the IUT_a and IUT_b respectively. In the following, simulation results are described. They have been obtained by taking into account sinusoidal laws as target time histories of the table displacement. These are characterized by a frequency of 0.5 and 1 Hz. The amplitude value has been chosen in accordance with the geometric properties of the isolator whereas the test frequencies have been selected in the typical working field of the base isolation devices under seismic action.

A. Testing of the IUT_a equipped test rig

Two sinusoidal target time histories, both characterized by an amplitude of 0.02 m, have been assigned. The tests have been realized at a supply pressure of 100 bar.

The illustrated results consist of comparison between the target and the effective displacement, control action, tracking error ($y - y_m$) and trajectory tracking error ($y - r$).

The results highlight the effectiveness (Fig. 15, 19) of the adaptive control which design is based on the first order non-linear system assumed as plant. After a transient characterised by the controller adaptation, the control action (Fig. 16, 20) determines a tracking error (Fig. 17, 21) and a trajectory tracking error (Fig. 18, 22) both converging to zero: it appears manifest the controlled system capability of following the reference model and, consequently, the target displacement. Furthermore, the target displacement amplitude is effected by the controlled system assuring the correct isolator testing. Even if the adaptation stage goes on asymptotically (Fig. 17, 18, 21, 22), the controller performance is fully satisfactory starting from the first seconds of the test.

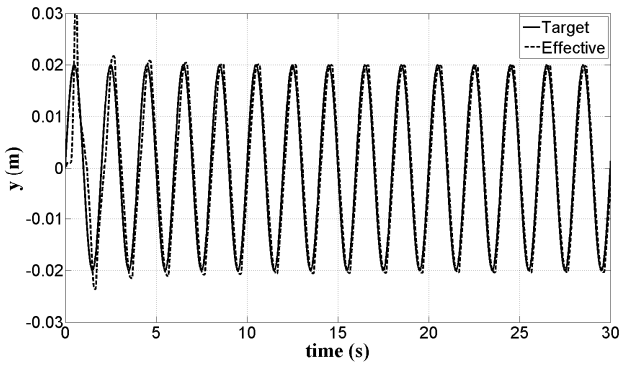

Fig. 15. Target vs effective displacement (0.5 Hz)

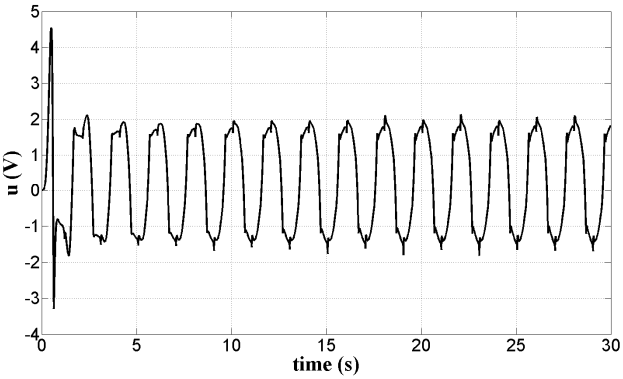

Fig. 16. Control action (0.5 Hz)

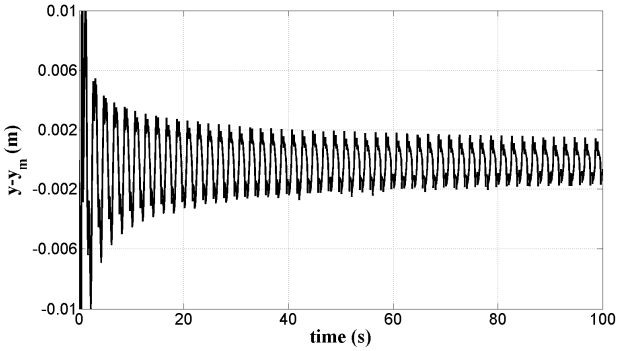

Fig. 17. Tracking error (0.5 Hz)

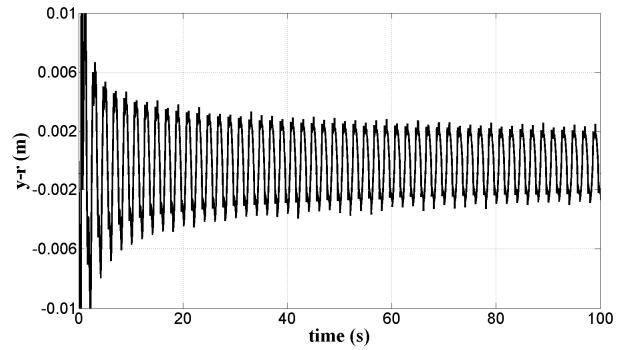

Fig. 18. Trajectory tracking error (0.5 Hz)

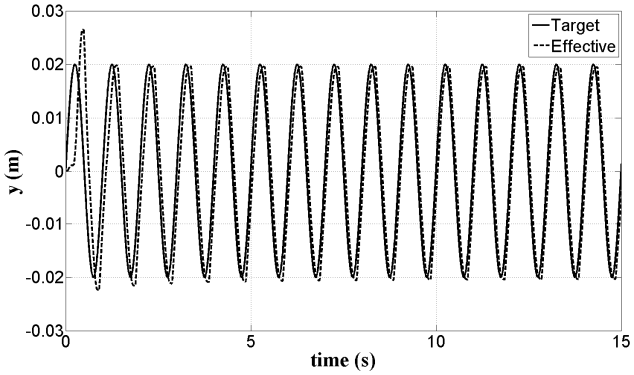

Fig. 19. Target vs effective displacement (1 Hz)

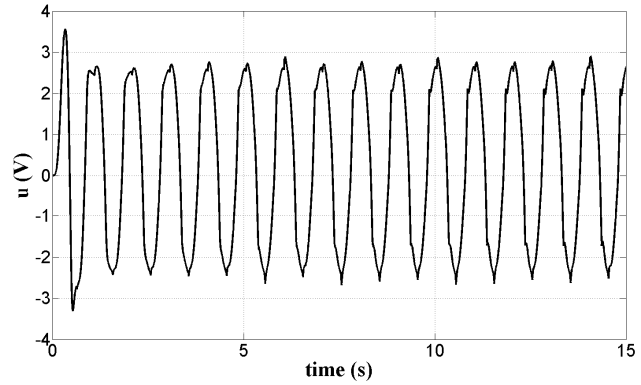

Fig. 20. Control action (1 Hz)

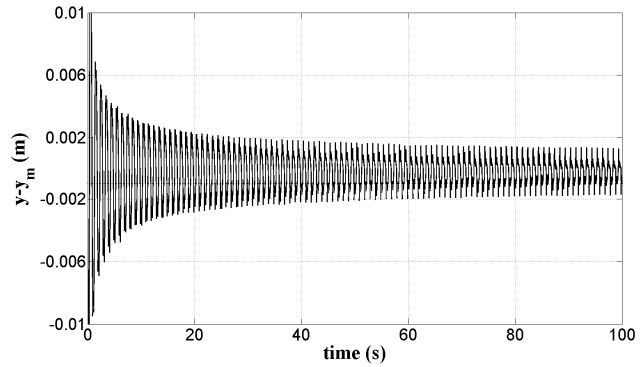

Fig. 21. Tracking error (1 Hz)

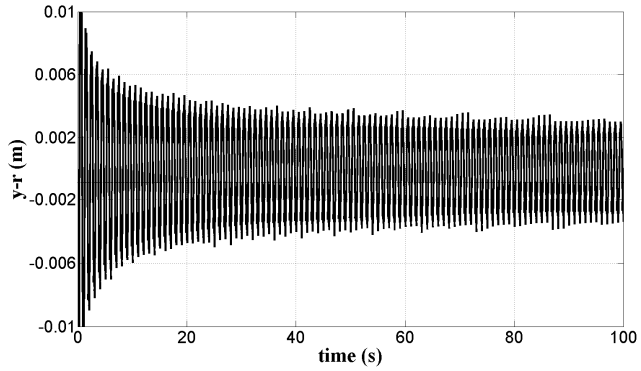

Fig. 22. Trajectory tracking error (1 Hz)

B. Testing of the IUT_b equipped test rig

The following results refer to the 5thOM in which the IUT_b has been considered. As already described, it consists in a device very different from the IUT_a as can be observed analyzing its parameters. In this way, the controller capability of adaptively making the tracking error convergent towards zero is tested in presence of a modified plant always characterized by unknown parameters. Two sinusoidal target time histories, both characterized by an amplitude of 0.03 m, have been assigned. The tests have been realized at a supply pressure of 70 bar.

The comparison between the target and the effective displacement (Fig. 23, 27) confirms the effectiveness of the proposed non-linear adaptive controller which, by means of the control action (Fig. 24, 28), is able to adaptively control the displacement in presence of a modified plant to be controlled. The tracking error (Fig. 25 and 29) and the trajectory tracking error (Fig. 26 and 30) illustrate are converging towards zero for both the adopted frequencies.

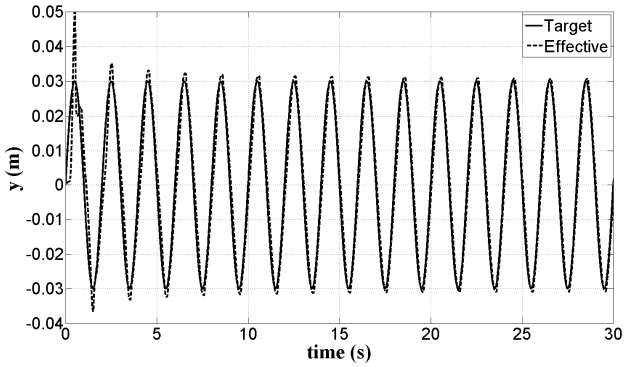

Fig. 23. Target vs effective displacement (0.5 Hz)

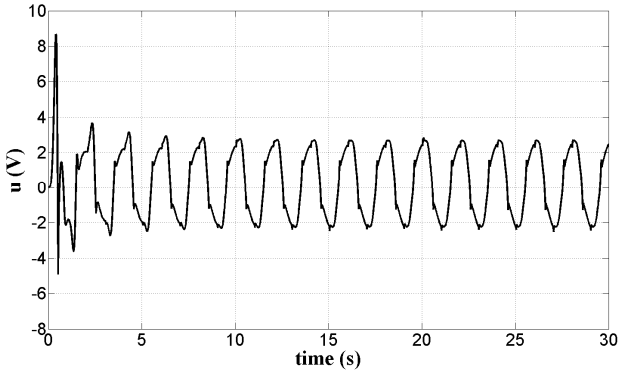

Fig. 24. Control action (0.5 Hz)

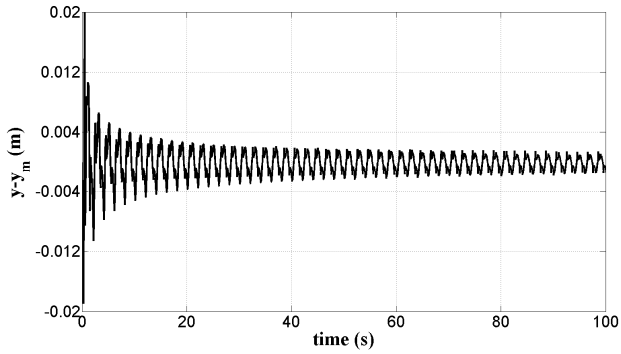

Fig. 25. Tracking error (0.5 Hz)

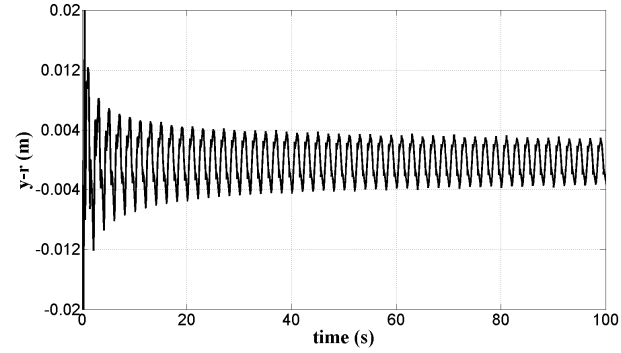

Fig. 26. Trajectory tracking error (0.5 Hz)

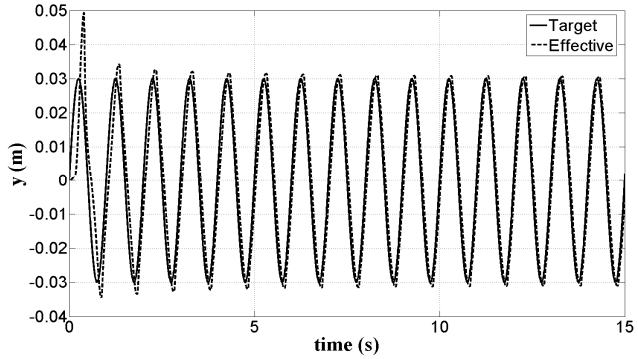

Fig. 27. Target vs effective displacement (1 Hz)

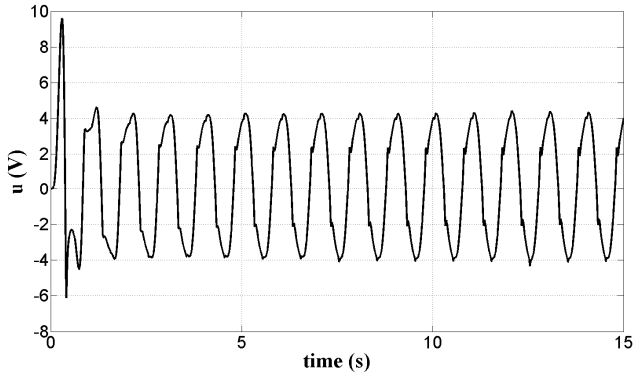

Fig. 28. Control action (1 Hz)

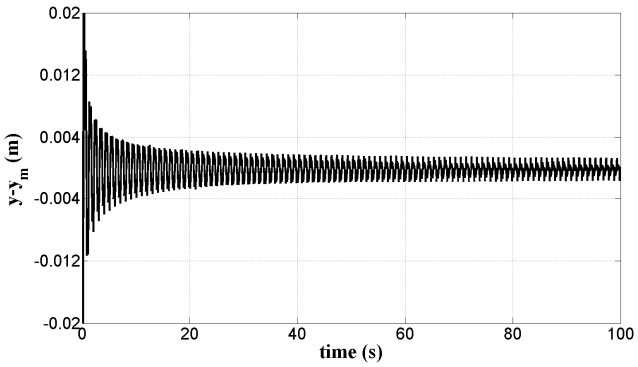

Fig. 29. Tracking error (1 Hz)

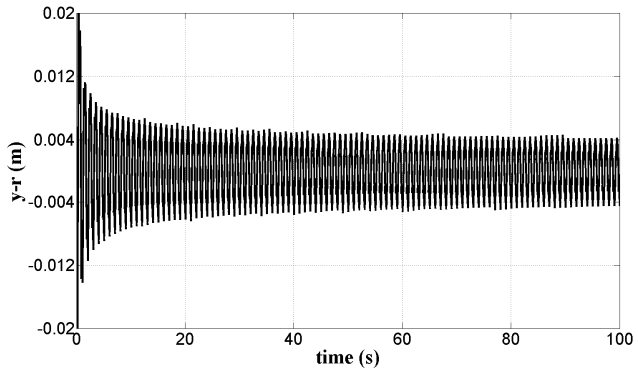

Fig. 30. Trajectory tracking error (1 Hz)

The described results fully validate the proposed approach for the position control synthesis of a hydraulic actuator employed as seismic isolator test rig. The designed regulator doesn't request any previous identification procedure and gives a control algorithm able to handle the parametric uncertainties that are typical in a testing machine finalized to test isolator with different characteristics. Furthermore, the adaptive controller well manages the 5thOM hard non-linearities due to dead zone and frictions.

VI. Conclusion

An experimental/theoretical activity has been carried out on a hydraulically actuated seismic isolator testing machine. The plant consists of a hydraulically actuated unidirectional moving platform on which a seismic isolator can be installed. A system structure identification procedure has been executed and a first order non-linear model derived. Taking into account the parametric uncertainty caused by the operating conditions and the unknown properties of the isolator to test, an adaptive approach has been adopted for the position controller synthesis. Starting from the reduced order system, the design procedure generated a non-linear adaptive control. Numerical simulations have been performed in order to test the developed control combined with the complete fifth order model of the plant. The illustrated results highlight the effectiveness of the designed controller in terms of tracking error and validate the proposed design procedure which allows to test different isolators without any previous identification procedure or controller tuning.

References

[1] J.S. Hwang, J.D. Wu, T.C. Pan and G. Yang, "A Mathematical Hysteretic Model for Elastomeric Isolation Bearings," *Earthquake Engineering and Structural Dynamics*, vol. 31, no. 4, pp. 771 – 789, Apr. 2002.

[2] I. I. Lazaro, A. Alvarez, and J. Anzurez, "The Identification Problem Applied to Periodic Systems Using Hartley Series," *Engineering Letters,* vol. 21, no.1, pp. 36 - 43, Feb. 2013.

[3] R. S. Schittenhelm, Z. Wang, B. Riemann, and S. Rinderknecht, "State Feedback in the Context of a Gyroscopic Rotor using a Disturbance Observer," *Engineering Letters,* vol. 21, no.1, pp. 44 - 51, Feb. 2013.

[4] R. Russo, M. Terzo, "Design of an adaptive control for a magnetorheological fluid brake with model parameters depending on temperature and speed," *Smart Materials and Structures*, vol. 20, no. 11, 115003, Nov. 2011.

[5] R. Russo, M. Terzo, "Modelling, parameter identification, and control of a shear mode magnetorheological device," *Proc IMechE Part I: Journal of Systems and Control Engineering*, vol. 225, no. 5, pp. 549–562, Aug. 2011.

[6] S. Pagano, R. Russo, S. Strano, M. Terzo, "Non-linear modelling and optimal control of a hydraulically actuated seismic isolator test rig," *Mechanical Systems and Signal Processing,* vol. 35, no. 1 – 2, pp. 255-278, Feb. 2013.

[7] S. Pagano, R. Russo, S. Strano, M. Terzo, "Modelling and Control of a Hydraulically Actuated Shaking Table Employed for Vibration Absorber Testing," in *Proc. of the ASME 11th Biennial Conference on Engineering Systems Design and Analysis (ESDA2012)*, vol. 1, 2012, pp. 651 – 660.

[8] M. Cardone, S. Strano, "Fluid-Dynamic Analysis of Earthquake Shaking Table Hydraulic Circuit," in *Proc. of the ASME 11th Biennial Conference on Engineering Systems Design and Analysis (ESDA2012)*, vol. 2, 2012, pp. 343 – 350.

[9] G. Di Massa, S. Pagano, E. Rocca, S. Strano, "Sensitive equipments on wrs-btu isolators," *Meccanica*, DOI: 10.1007/s11012-013-9708-9, 2013.

[10] M. Dolce, D. Cardone, "Theoretical and experimental studies for the application of shape memory alloys in civil engineering", *Journal of Engineering Materials and Technology*, vol. 128, no. 3, pp. 302 – 311, 2006.

[11] R. Haber, L. Keviczky, , *Nonlinear system identification- Input-Output modeling approach*, Netherlands, Kluwer Academic Publishers, 1999.

[12] R. De Rosa, M. Russo, R. Russo, M. Terzo, "Optimisation of handling and traction in a rear wheel drive vehicle by means of magneto-rheological semi-active differential," *Vehicle System Dynamics*, vol. 47, no. 5, pp. 533 – 550, May 2009.

[13] J.J.E. Slotine, W. Li,. *Applied Nonlinear Control*, NJ, Prentice Hall, 1991.